Interdiffusion effect on the gain of InGaAs/InP quantum well laser

Michael CY Chan[1], K.S.Chan[2] and E Herbert Li[1]
[1] Department of Electrical and Electronic Engineering, The University of Hong Kong
[2] Department of Physics and Materials Science, City University of Hong Kong

ABSTRACT

Lattice-matched $In_{0.53}Ga_{0.47}As/InP$ quantum well (QW) structures are of considerable interest in photonic application since they enabled device operation in the 1.3μm to 1.55μm wavelength range which is of importance for optical communication systems.

The process of interdiffusion modifies the as-grown square QW to a graded QW which alter the subband structure and optical properties of the QW. Thus it provides a useful tool for bandstructure engineering. The interdiffusion process of InGaAs/InP QW provides more degrees of freedom than AlGaAs/GaAs QW system since interdiffusion can occur for group-III (In, Ga), group-V (As, P), and groups III plus V together. These are determined by the temperature and chemical environment used during annealing of the QW structure.

The effect of interdiffusion on the laser performances of InGaAs/InP QWs is also studied base on these different types of diffusion processes. It is found that the operating wavelength shows both a red shift and a blue shift depending on the types of diffusion process. It is also found that group-III interdiffusion gives the best performance of InGaAs/InP QW laser when comparing to the other two types of interdiffusion in terms of a smaller threshold carrier density.

Keywords: interdiffusion, bandstructure engineering, InGaAs/InP, laser gain, quantum well

1. INTRODUCTION

Currently InGaAs/InP quantum-well (QW) structures are actively studied for the fabrication of a variety of optoelectronic devices, such as modulators, detectors, waveguides, and lasers, for operation in the 1.3μm-1.55μm wavelength region[1-3]. By exploiting the strain effects on the band-gap, the bandstructure of the device can be engineered to optimize the device characteristics. Apart from this, interdiffusion of constituent atoms, the rate of which depends on lattice distortion, impurities, defects and the process temperature, is a versatile technique to modify the device bandstructure. Using this technique, the QW compositional profile, the confinement potential and the optical properties can be modified as a result of the diffusion of constituent atoms. The interdiffusion processes in InGaAs/InP QW system is more complex than those in AlGaAs/GaAs and InGaAs/GaAs because both group-III and group-V atoms can participate in the interdiffusion process. The interdiffusion of InGaAs/InP QW structures induced by

 0-8194-2287-8/96/$6.00

means of various techniques such as impurities induced diffusion and impurity-free vacancy diffusion is being widely investigated experimentally.[4-11] The results obtained have been interpreted in terms of different interdiffusion process taking place as a result of the disordering process and the impurity species used. The reported results can be grouped into three interpretations: i) comparable interdiffusion rates on both group III and group V sublattices; ii) group III sublattice interdiffusion only; iii) interdiffusion on both sublattices, but with different interdiffusion rates. Therefore it is important to understand the effects of interdiffusion on the optical characteristic of InGaAs/InP QWs for integration and optimization of devices.

In this paper, we model the interdiffusion process in an undoped InGaAs/InP single QW and study the effects of interdiffusion on the optical gain of the interdiffused QW lasers. In section 2 we briefly discuss the models of group III and group V interdiffusion. In section 3 we present the model for the calculation of the band structure and the optical gain of strained QW structures. In sections 4 and 5, we discuss the interdiffused confinement profile and the optical gain of interdifffused InGaAs/InP QW lasers. A conclusion is given in section 6.

2. MODEL OF INTERDIFFUSION

In the present work we considered the following interdiffusion processes: (i) group III sublattice only; (ii) both group III and group V sublattices with the same interdiffusion rates; and (iii) group V sublattice only. For case (i) and (ii), the interdiffusion processes are assumed to be one phase in which the concentration is continuous across the interface and the diffusion constant is constant throughout the heterostructure. For case (iii), the study of Mukai *et al*[11] shows that the interdiffusion process is a two phase process in which the concentration is discontinuous across the interface and the diffusion constant is not a constant throughout the whole heterostructure.

2.1 One phase diffusion

It is assumed that the group-III and group-V interdiffusion processes are independent of each other and are modeled by two different diffusion length. The interdiffusion of In and Ga atoms is charaterized by a diffusion length L_d^{III}, which is defined as $L_d^{III}=\sqrt{(D^{III}t)}$, where D^{III} is the diffusion coefficient of group-III atoms and t is the diffusion time. The interdiffusion of As and P atoms is characterized by the diffusion length L_d^{V}. The structure to be modeled consists of an as-grown $In_{0.53}Ga_{0.47}As$ square well sandwiched between two thick InP barriers. After intermixing, the concentration of the interdiffused atoms across the QW structure is determined by solving the diffusion equation and the In concentration after interdiffusion is given by

$$x_{In}(z) = 1 - \frac{1-x}{2}\left[\mathrm{erf}\left(\frac{L_z + 2z}{4L_d^{III}}\right) + \mathrm{erf}\left(\frac{L_z - 2z}{4L_d^{III}}\right)\right] \quad (1)$$

where L_z is the as-grown well width, z is the growth direction, and the QW is centered at z=0. The As concentration after interdiffusion is given by

$$y_{As}(z) = \frac{y}{2}[\mathrm{erf}(\frac{L_z + 2z}{4L_d^V}) + \mathrm{erf}(\frac{L_z - 2z}{4L_d^V})]$$

where y is the As composition and equals 1 for the as-grown structure.

2.2 Two phase diffusion

According to the work of Mukai *et al*[11], the lattice distortion in a strained QW structure affects the diffusion process in such a way that concentrations of the constituent atoms are not continuous across the interface after interdiffusion. The concentrations across are related to each other by a constant ratio. Mukai have studied in details the diffusion of group V atoms in InGaAs/InP and obtained experimental values for the distribution ratio of concentration across the interface. In the two phase diffusion model, the interdiffusion process is described by a set of linear diffusion equations

$$\frac{\partial C_i(z,t)}{\partial t} = D_i \frac{\partial^2 C_i(z,t)}{\partial z^2} \qquad (2)$$

where i = b for the barrier region and is valid only for $t > 0$, $|z| > L$ or i = w for the well region and valid only for $t > 0$, $|z| < L$; C_i is the concentration of diffusion species in different layers; D_i is the diffusion coefficients of group-V atoms in different layers. The discontinuity of the concentration across the interface and the continuity of diffusion flux give the following boundary conditions

$$C_b(z,t)=kC_w(z,t)\,, \qquad z=\pm L \qquad (3)$$

and

$$D_w \frac{\partial C_w(z,t)}{\partial z} = D_b \frac{\partial C_b(z,t)}{\partial z}, \qquad z=\pm L \qquad (4)$$

where k is the interfacial distribution ratio of concentration. We solve the set of differential equations numerically using the finite difference method.

3. THEORY

3.1 Effects of strain

In the present work, we consider the interdiffusion of $In_{0.53}Ga_{0.47}As/InP$ QW, in which the quantum well layer is lattice-matched to the barrier layer. After interdiffusion, the chemical composition deviates from the lattice-matched condition leading to non-uniform strain and hence modified potential profile in the well and barrier region. The in-plane strain, $\varepsilon(x,y)$, varies across the whole heterostructure so the strain effects are also z-dependent. Assuming that the growth direction z is along <001>, then the biaxial strain components parallel to the interface after interdiffusion are given by:

$$\varepsilon_{xx} = \varepsilon_{yy} = \varepsilon(x,y) \quad (5)$$

$$\varepsilon_{zz} = -2[c_{12}(x,y)/c_{11}(x.y)]\varepsilon(x,y) \quad (6)$$

$$\varepsilon_{xy} = \varepsilon_{yz} = \varepsilon_{zx} = 0 \quad (7)$$

where $\varepsilon(x,y)$ is defined to be negative for compressive strain, and $c_{ij}(x,y)$ are the elastic stiffness constants. The change in the bulk bandgap, $S_{\perp}(x,y)$, due to the biaxial component of strain is given by[12]:

$$S_{\perp}(x,y) = -2a(x,y)[1-c_{12}(x,y)/c_{11}(x,y)]\varepsilon(x,y) \quad (8)$$

where a(x,y) is the hydrostatic deformation potential calculated from:

$$a(x,y) = -\frac{1}{3}[c_{11}(x,y) + 2c_{12}(x,y)]\frac{dE_g(x,y)}{dP} \quad (9)$$

where dE_g/dP is the hydrostatic pressure coefficient of the lowest direct energy gap E_g. The splitting energy, $S_{//}(x,y)$, between the HH and LH band edges induced by the uniaxial component of strain is given by:

$$S_{//}(x,y) = -b(x,y)[1+2c_{12}(x,y)/c_{11}(x,y)]\varepsilon\,(x,y) \quad (10)$$

where b(x,y) is the shear deformation potential. The parameters a,b,c_{ij}, dE_g/dP in above equations are assumed to obey Vegard's law, so that their respective values depend directly on the compositional profiles across the QW. The LH and spin-orbit split-off band are coupled due to the presence of strain while the HH state and spin-orbit split-off band remains uncoupled. The valence band splitting at Γ for the HH band and for the LH band are given by[13]:

$$S_{//HH}(x,y)=S_{//}(x,y) \quad (11)$$

$$S_{//LH}(x,y)=-[S_{//}(x,y)+\Delta_o(x,y)]/2+[9\{S_{//}(x,y)\}^2+\{\Delta_o(x,y)\}^2-2S_{//}(x,y)\Delta_o(x,y)]^{1/2}/2 \quad (12)$$

respectively, where $\Delta_o(x,y)$ is the spin-orbit splitting. The QW confinement potential after the disordering process, $U_r(x,y)$, is obtained by summing the unstrained potential profile after processing, $\Delta E_r(x,y)$ and the potential due to strain

$$U_r(x,y)=\Delta E_r(x,y)- S_{\perp r}(x,y)\pm S_{//r}(x,y) \quad (13)$$

where $S_{\perp r}(x,y)=Q_r S_{\perp}(x,y)$, the '+' and '-' signs represent the confined HH and LH profiles,respectively, and $S_{//c}(x,y)=0$. Q_r (r=C,V) is the band offset ratio for the conduction and valence bands.

3.2 Bandstructure

To calculate the electron and hole wave function in QW, we use the multiband effective mass theory. For most III-V semiconductors such as GaAs-based materials, it is a good approximation that the conduction and valence bands are decoupled. A simple isotropic parabolic band is used for the conduction band, and a 4×4 Luttinger-Kohn Hamiltonian with the strain components is used for the valence band. The electron states near the conduction subband edge are assumed to be almost purely s-like and nondegenerate (excluding spin), while the hole states near the valence subband edge are almost purely p-like and four-fold degenerate (including spin). The envelope function scheme is adopted to describe the slowly varying (spatially extended) part of the wavefunction.

The envelope function of the electron and hole wavefunction at the subband edge ($k_{//}=0$, $k_{//}$ denotes the wavevector in the x-y plan) can be calculated separately using the one-dimensional Schrödinger-like equation as follows

$$-\frac{\hbar^2}{2}\frac{d}{dz}\left[\frac{1}{m^*_{\perp r}(z)}\frac{d\psi_{rl}(z)}{dz}\right]+U_r(z)\cdot\psi_{rl}(z)=E_{rl}\psi_{rl}(z) \quad (14)$$

where $\psi_{ri}(z)$ is the envelope function of the l^{th} subband for electron or hole (r=c for electrons and r=v for holes). $m^*_{\perp r}(z)$ is the corresponding carrier effective mass in the z direction and E_{ri} is the subband-edge energy. Equation (14) is solved numerically using the finite difference method with an appropriate confinement profile.

For valence subband structure, it is necessary to diagonalize the Luttinger-Kohn Hamiltonian with appropriate confinement potentials for heavy and light holes. The envelope functions at finite $k_{//}$ depend on $k_{//}$ as a result of the mixing of the heavy and light hole bands. In the present work, we use the effective Hamiltonian approach described in Chan[14] to calculate the valence subband structure. In this approach, the hole envelope function $\psi_{vl}(k_{//},z)$ at any finite $k_{//}$ which is not too far away from the Brillouin zone centre

($k_{//}$=0) can be expressed as a linear combination of the envelope functions $\psi_{vl}(z)$ at $k_{//}$=0 as follows

$$\psi(k_{//},z)=\sum_{l=1}^{N}\sum_{v=-3/2}^{3/2} d_{v,l}(k_{//})\cdot\psi_{v,l}(z) \qquad (15)$$

$\psi_{vl}(z)$ are obtained by solving equation (14). This approximation is accurate within a limited range of $k_{//}$, as only a finite basis set is used in the linear expansion. A basis set of about 40 envelop functions is used in the present calculation and the results obtained are accurate within the operation energy range of QW laser. The effect Hamiltonian obtained is

$$\begin{bmatrix} E_{3/2}+S_{//HH} & C & B & 0 \\ C^* & E_{-1/2}-S_{//LH} & 0 & B^T \\ B^* & 0 & E_{+1/2}-S_{//LH} & C^T \\ 0 & B^* & C^* & E_{-3/2}+S_{//HH} \end{bmatrix} \qquad (16)$$

where C, B, and E are submatrices of the Hamiltonian matrix with matrix elements given below

$$C_{rs}=\left[\frac{3}{4}\right]^{1/2}\frac{\hbar^2}{m_o}\gamma_2(k_x-ik_y)^2\int_{-\infty}^{\infty}dz\psi_{-3/2,r}(z)\psi_{1/2,s}(z)$$

$$B_{rs}=3^{1/2}\frac{\hbar^2}{m_o}\gamma_2(-k_x-ik_y)\int_{-\infty}^{\infty}dz\psi_{3/2,r}(z)\frac{\partial}{\partial z}\psi_{-1/2,s}(z)$$

$$E_{\pm3/2,ss'}=\delta_{ss'}E_{Hs}-\frac{\hbar^2}{2m_{//H}}k_{//}^2$$

$$E_{\pm1/2,ss'}=\delta_{ss'}E_{Ls}-\frac{\hbar^2}{2m_{//L}}k_{//}^2$$

γ_2 is the Luttinger-Kohn parameter.

3.3 Optical gain

The optical gain spectra are calculated by the density matrix approach and the gain due to the transition between the conduction subband p and the valence subband q is given by

$$g_{pq}(E) = \frac{2\pi q^2 \hbar}{(2\pi)^2 n\varepsilon_0 c m_0^2 L_w E} \cdot \int dk \left|\hat{e} \cdot P_{pq}(k_{//})\right|^2 \rho\left(E_p^e(k_{//}) - E_q^h(k_{//}) - E\right) \times\left[f^e\left(E_p^e(k_{//})\right) - f^h\left(E_q^h(k_{//})\right)\right] \quad (17)$$

where q is the electric charge, n is the refractive index, ε_0 is the dielectric constant of the vacuum, c is the speed of light, L_w is the width of the quantum well, E is the photon energy, P_{pq} is the optical matrix element, $\hat{e}$ is a unit vector along the polarization direction of the optical electric field, and f^e and f^h are the Fermi distribution function for electron in the conduction and valence subband, respectively. To include the spectral broadening of each transition, the total gain is convoluted with Lorentzian lineshape function over all transition energies E'.

$$G(E) = \int dE' \sum_{p,q} g_{pq}(E') L(E - E') \quad (18)$$

where L(E-E') is given by

$$L(E - E') = \frac{1}{\pi} \frac{\hbar / \tau_{in}}{(E'-E)^2 + (\hbar / \tau_{in})^2} \quad (19)$$

τ_{in} is the intraband relaxation time.

4.CONFINEMENT POTENTIAL

4.1 Group III diffusion only

We show the confinement potentials of electrons and hole in figure 1. The effective barrier heights of the confinement potentials are increased by interdiffusion, which results in strain build-up around the interface. When Ga atoms diffuse into the InP barrier and In atoms diffuse into the QW, an InGaP/InGaAs interface is formed. The distribution of the In and Ga atoms are described by the error function distribution, while the As and P concentration profiles do not change. Since the InP lattice constant is always larger than that of InGaP, a tensile strain arises in the barrier near the interface, while the InGaAs well becomes compressively strained due to the increase in In content. Consequently the disordering process results in a strained QW structure. The strain affects the shape and the separation of the conduction and valence bands, and the HH and LH potential well no longer coincide. The confinement profile of the interdiffused structure remains abrupt with width equal to that of the as-grown QW. The effective well bottom of electrons and heavy holes are lowered as a result of interdiffusion, which gives rise to band-gap shifting to longer wavelength.

4.2 Both group III & V diffusion

In the present work, we assume the rates of interdiffusion for the two sublattices are comparable and leave the case of different rates of interdiffusion to subsequent work. When both sublattices diffuse at the same rate, the structure remains lattice matched and there is no strain through out the QW structure. As shown in figure 2 the confinement potentials have error function profiles. In contrast to the case of group III diffusion only, the potential profile after interdiffusion are no longer abrupt and the HH and LH profiles still coincides since no strain is present. The transition energies of C1-HH1 and C1-LH1 transitions increases as interdiffusion proceeds, which results in a band-gap shift to shorter wavelength.

4.3 Group V diffusion only

The confinement profiles of the interdiffused QW for considering only group V diffusion is shown in figure 3. We use a two phase diffusion model to describe the interdiffusion process. The model parameters we used are those for 650°C obtained by Mukai for $In_{0.53}Ga_{0.47}As/InP$ QW. The diffusion constant is $2.1x10^{-17}cm^2/s$ in InGaAs and is $2.1x10^{-19}cm^2/s$ in InP. The diffusion rate of group V atoms inside the well layer is about two orders of magnitude larger than that in the barrier layer. This results in a nearly flat potential profile inside the well and a graded potential in the barrier layer. The distribution ratio of group V atoms between the barrier and the well is 30, which is quite large. As a result, the confinement potentials always remain abrupt even after significant interdiffusion.

5. OPTICAL GAIN

The gain results of interdiffused lattice-matched InGaAs/InP QW for different diffusion processes are shown in figure 4. The carrier density used in the calculation is $5x10^{12}cm^{-2}$. In figure 4 (a), we show the gain of quantum wells with interdiffusion of only group III sublattice. The peak gain energy shifts to lower energies as interdiffusion proceeds and the peak gain magnitude increases with the degree of interdiffusion. This is due to the deepening of the QW potential and the increase in confinement when the group III atoms interdiffuse. Figure 4(b) shows the gain after interdiffusion of group V sublattice. We notice that the peak gain energy shifts to higher energies when the well is interdiffused. Nevertheless the magnitude of energy shift is much smaller than that in group III diffusion, which is due to the large distribution ratio across the interface resulting in a small change in confinement potential inside the well. The gain of well with interdiffusion of both group III and group V sublattices are shown in figure 4(c). The error function confinement profile of this kind of interdiffused quantum well shifts the peak of the gain spectrum to high energies and reduces the peak height.

6. CONCLUSION

The effects on the gain spectrum of a lattice-matched InGaAs/InP quantum well laser due to interdiffusion depend on the interdiffusion process involved. It is shown that

the interdiffusion of group III sublattice can lead to an increase in the peak gain and hence a reduction in operation current.

7. ACKNOWLEDGEMENT

This work is supported in part by the CityU strategic research grant, RGC earmarked grant and HKU-CRCG grant..

8. REFERENCES

1. R.J. Deri, E.Kapon, R.Bhat, M.Seto and K.Kash, Appl. Phys. Lett., Vol.54, pp.1737, 1989.
2. I.Bar-Joseph, C.Klingshirn, D.A.B.Miller, D.S.Chemla, U.Koren and B.I.Miller, Appl. Phys. Lett., vol.50 pp.1010, 1987.
3. U.Koren, B.I.Miller, T.L.Koch, G.Eisenstein, R.S.Tucher, I.Bar-Joseph and D.S.Chemla, Appl. Phys. Lett., vol.51, pp.1132, 1987.
4. B.Tell, J.Shah, D.M.Thomas, K.F. Brown-Goebeler, A.DiGiovnni, B.I.Miller and U.Koren, Appl. Phys. Lett. vol.54, pp.1570, 1989.
5. H.Sumida, H.Asahi, S.J.Yu, K.Asami, S.Gonda and H.Tanoue, Appl. Phys. Lett. vol.54, pp.520, 1989.
6. I.J.Pape, P.Li Kam Wa, J.P.R.David, P.A.Claxton, P.N.Robson and D.Sykes, Electron. Lett. vol.24, pp.910, 1988.
7. K.Nakashima, Y.Kawaguchi, Y.Kawamura, Y.Imamura and H.Asahi, Appl. Phys. Lett., vol.52, pp.1383, 1988.
8. S.A.Schwarz, P.Mei, T.Venkatessen, R.Bhat, D.M.Hwang, C.L.Schwarz, M.Koza, L.Nazar and B.J.Skromme, Appl. Phys. Lett. vol.53, pp.1051, 1988.
9. I.J.Pape, P.Li Kam Wa, J.P.R.David, P.A.Claxton and P.B.Robson, Electron. Lett., vol.24, pp.1217, 1988.
10. T.Miyazawa, H.Iwamura, O.Mikami and M.Naganuma, Jpn. J. Appl. Phys. vol.18, pp.L1030, 1989.
11. K.Mukai, M.Sugawara and S.Yamazaki, Phys. Rev. B, vol.50, pp.2273, 1994.
12. H.Asai and K.Oe, J. Appl. Phys., vol.54, pp.2052, 1983.
13. R.People, Phys. Rev. B, vol.32, pp.1405, 1985.
14. K.S.Chan, J. Phys. C: Solid State Phys., vol.19, pp.L125, 1986.

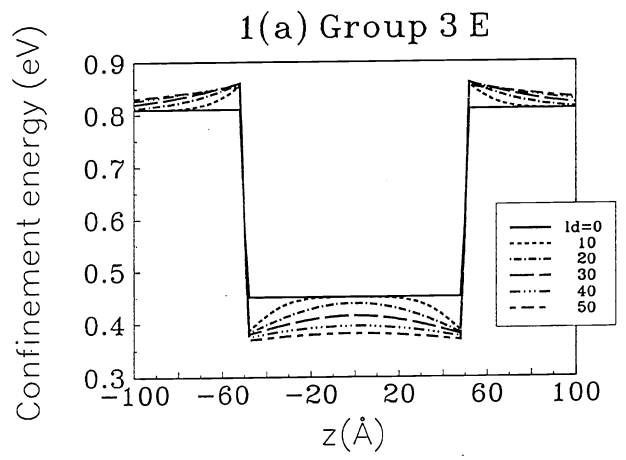

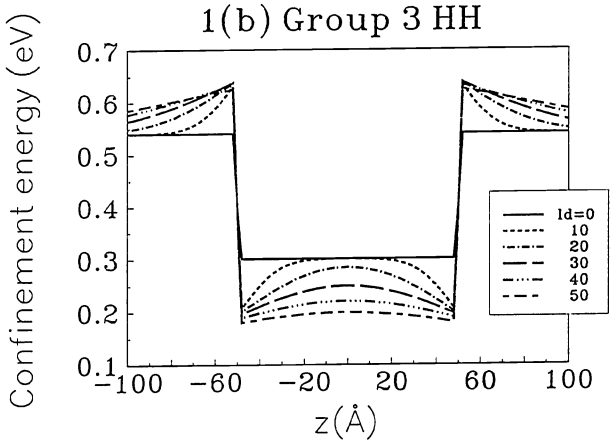

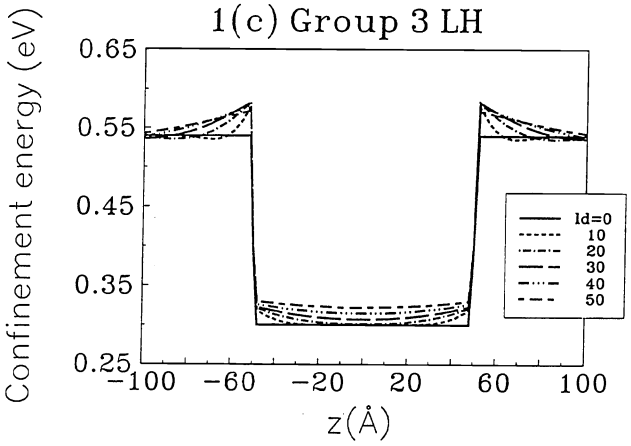

Figure 1 Confinement potential: Group III diffusion only; (a) electron (b) heavy hole (c) light hole

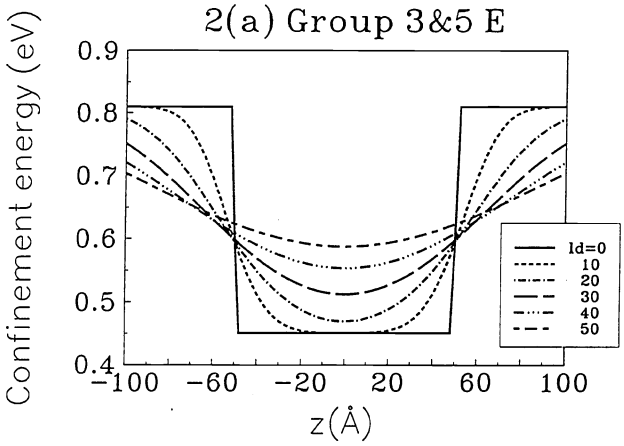

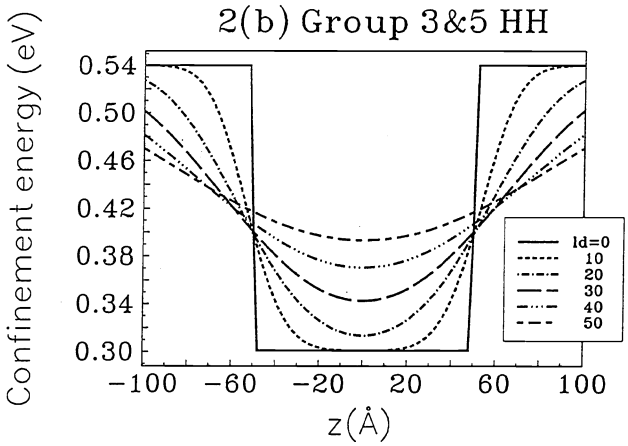

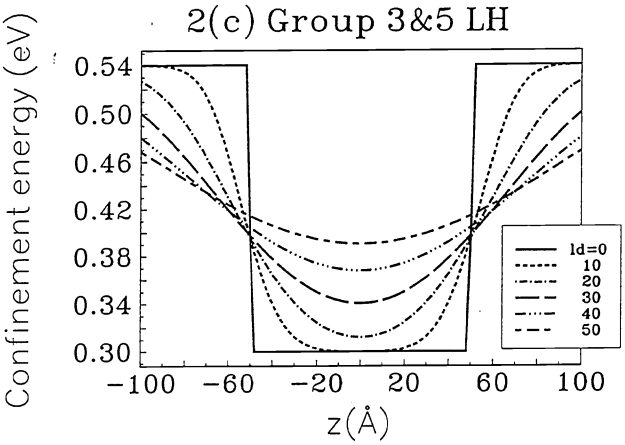

Figure 2 Confinement potential: Group III &V diffusion; (a) electron (b) heavy hole (c) light hole

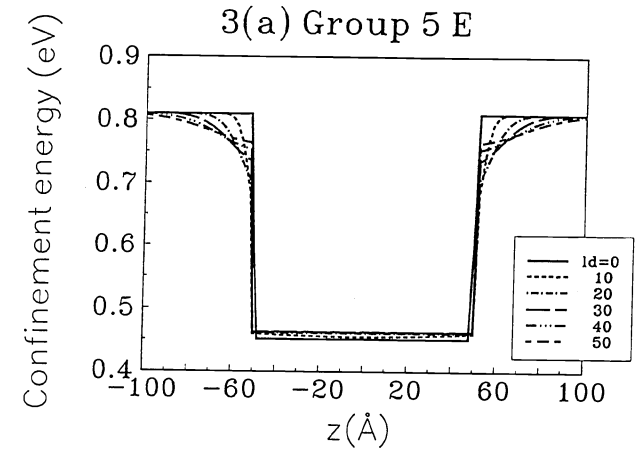

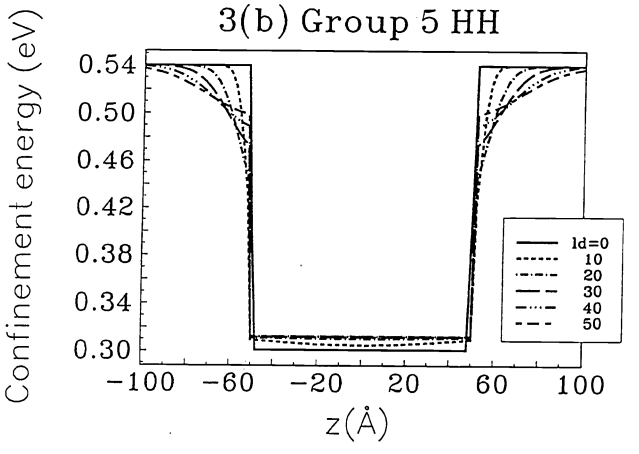

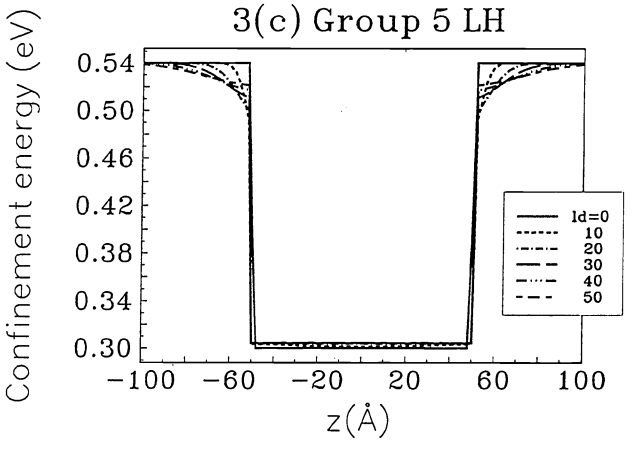

Figure 3 Confinement potential Group V diffusion (a) electron (b) heavy hole (c) light hole

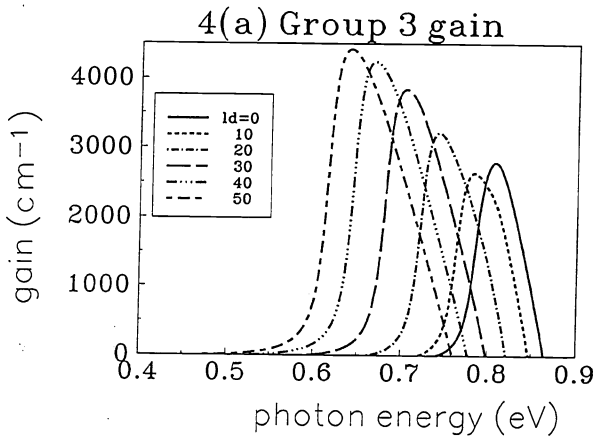

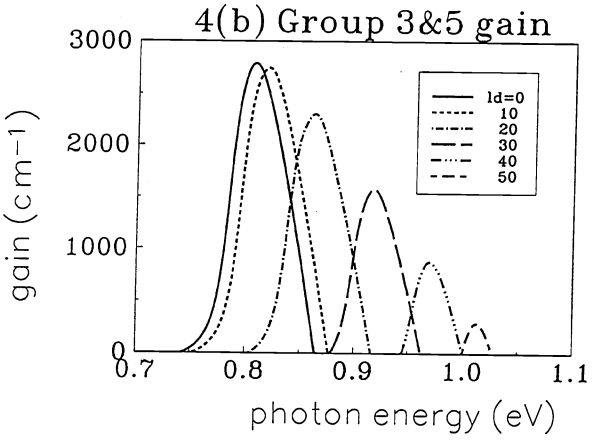

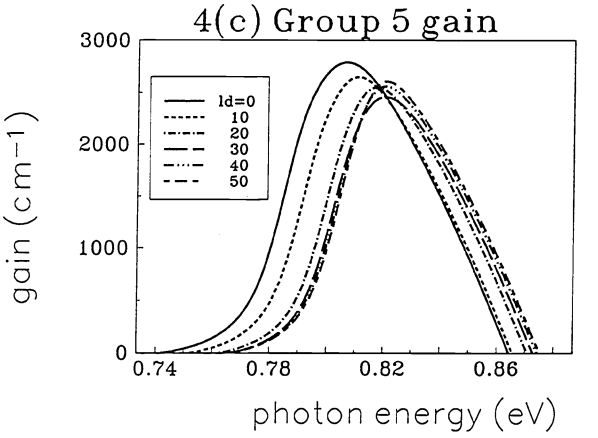

Figure 4 Gain (a) Group III diffusion (b) Group III & V (c) Group V only